

# ON THE VARIABILITY OF SATURN'S EQUATORIAL JET AT CLOUD TOP LEVEL

AGUSTÍN SÁNCHEZ-LAVEGA, RICARDO HUESO, SANTIAGO  
PÉREZ-HOYOS

*Grupo Ciencias Planetarias, Departamento Física Aplicada I, Escuela Técnica  
Superior de Ingeniería, Universidad del País Vasco, Bilbao, SPAIN.*

**Abstract:** Saturn's Equatorial jet is apparently highly variable in wind speed at the upper cloud level with changes, between 1980-81 and 1994-2004, amounting up to a 40% in its peak value. However, there is some controversy if this is a real change in the winds or an effect due to clouds placed at different altitude levels where a vertical wind shear is present. In a recent study of cloud altitudes we have shown [1] that vertical shears alone cannot account for the  $200 \text{ m s}^{-1}$  velocity change observed between both periods. Here, we reinforce this hypothesis based on simple dynamical calculations and discuss possible phenomena that can be involved in such variability.

## 1 Introduction

The strong eastward equatorial jets in the upper cloud level of Jupiter (jet meridional extent  $\sim \pm 10^\circ$  and speeds  $100 - 125 \text{ m s}^{-1}$ ) and Saturn (extent  $\sim \pm 40^\circ$  and speed ranging from  $275$  to  $475 \text{ m s}^{-1}$ ), represents a challenge for atmospheric modelling, and their dynamical origin remains an unsolved problem [2, 3, 4]. Quantification of the degree of variability of the jets is an important aspect to make an assessment between the extreme opposed models so far proposed to explain the nature of the atmospheric circulation of these planets. For example, focusing on Saturn, and within the context of "shallow layer models", one should expect large sensitivity to meteorology and to the seasonal insolation cycle in particular at Equatorial latitudes where sunlight seasons are enhanced by ring shadowing [5]. The same should occur on the recently proposed combined mechanisms of a Hadley circulation and a Kelvin wave to produce the equatorial [6]. On the contrary, zonal jets are expected to show little temporal variability if they are deeply rooted ([7] and references therein). On Saturn, the observations from ground-based telescopes, Voyagers 1 and 2, Hubble Space Telescope (HST)

and Cassini spacecrafts, point towards the stability of the zonal jet system outside the central equatorial area (i.e. poleward of latitudes  $\pm 20^\circ$ ). But between  $20^\circ$  N and  $20^\circ$  S, it has been recently reported a great variability, up to  $200 \text{ m s}^{-1}$  in the Equatorial Jet intensity between the Voyagers observations in 1980-81 and the HST data for 1994-2004 [8]. This change took place after a huge storm, a "Great White Spot" (GWS), which developed in 1990 [9, 10]. The jet speed variability has been confirmed by cloud tracking on Cassini images following the orbital injection of the spacecraft in July 2004 [11]. In particular, their data show wind speeds at the Equator that depend on the filter used to detect the cloud tracers (methane band at  $727 \text{ nm}$  and adjacent continuum at  $752 \text{ nm}$ ). The  $727 \text{ nm}$  cloud tracking data (sensitive to a high altitude within the clouds), agree with the HST velocity profile (jet peak velocities  $\sim 250 - 300 \text{ m s}^{-1}$ ), but the  $752 \text{ nm}$  (sensitive to lower altitudes) data give higher velocities ( $\sim 325 - 400 \text{ m s}^{-1}$ ; see Figure 1 of [11]) that are intermediate to those measured during the Voyager era (peak values of  $460 \text{ m s}^{-1}$  at  $7^\circ$  N, [13]). Accordingly, [11] favored the idea that the variability is in fact an apparent effect due to vertical wind shear in the jet and the different altitudes sensed by these filters. However, we have recently shown that this is not likely to be the case, based on a detailed study of cloud altitudes in the two different periods considered, 1980-81 and 1996-2004 [1].

The goal of this essay is first to show, in agreement with our photometric analysis, that the proposal of the "altitude effect" to explain wind differences is not compatible with the temperature measurements recently presented at the equator by two different teams. Therefore we present alternative dynamical mechanisms that could be involved in the jet variability at the tropopause level and quantify their effect on the wind velocities.

## 2 Sources of Variability

### 2.1 Altitude Effect: Vertical wind shears?

Our photometric analysis placed the cloud tracers sensed by HST and Cassini between  $\sim 50 \text{ mbar}$  and  $300 \text{ mbar}$  [1]. The measured velocities give a maximum vertical wind shear at  $3^\circ$  N between these levels of  $\partial u / \partial z = 46 \text{ m s}^{-1} / H$  ( $u$  is the zonal wind speed,  $z$  the vertical coordinate and  $H$  the scale height  $\sim 38 \text{ km}$  at the levels discussed in this paper). The wind shear problem comes when comparing Cassini-ISS  $750 \text{ nm}$  data and Voyager 1 & 2 data (always at the same latitude,  $3^\circ$  N) since the tracers were found at similar levels ( $\sim 300 - 400 \text{ mbar}$ ) but the speeds differed by  $100 \text{ m s}^{-1}$ . Even forcing the altitude error bars between both sets to the maximum altitude difference, the wind shear retrieved is

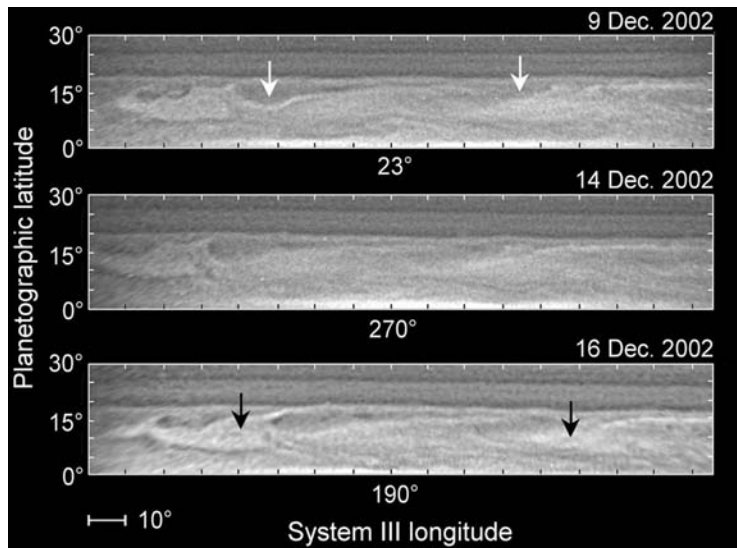


Figure 1: Cylindrical map projections of the Equatorial Zone as observed with the Hubble Space Telescope in December 2002 with the 890 nm (methane band) filter. The arrows mark the dominant wavenumber 2 for the larger dark and bright features.

extremely large,  $\partial u/\partial z \sim 200-350 \text{ ms}^{-1}/H$ . Note that the latitude consideration is important since the Voyager equatorial wind profile showed a large meridional wind shear [12, 13], not found in HST and Cassini data [8, 11, 14]. The above vertical shears derived from cloud tracking can be compared with those retrieved from the temperature measurements and the thermal wind equation for latitudes outside  $\pm 5^\circ$ . At the Voyager epoch, maximum wind shears were  $\partial u/\partial z \sim 30 \text{ ms}^{-1}/H$  at the 150 mbar level and latitudes  $10^\circ \text{ N}$  and  $10^\circ \text{ S}$  [15]. At the Cassini epoch, wind shears at latitudes  $5^\circ \text{ S} - 10^\circ \text{ S}$  were  $\partial u/\partial z = 15 \text{ ms}^{-1}/H$  above the 100 mbar level, and  $\partial u/\partial z = 45 \text{ ms}^{-1}/H$  above 500 mbar [16, 17]. Therefore cloud motions and thermal winds agree in the vertical wind shear estimations in the upper troposphere (300–500 mbar) at the Voyager, HST and Cassini epochs, to be  $\partial u/\partial z \sim 30 - 50 \text{ ms}^{-1}/H$ . However, the large vertical shear derived from a comparison between Voyager and HST-Cassini winds at 727 nm is 5–10 times the thermal wind shear. In other words, if thermal winds are assumed to be still the cause for the speed differences, a large meridional temperature gradient should exist in Saturn's equator. Let's estimate this thermal contrast. Using the beta-plane approximation for equatorial latitudes ( $f_0 = 2\Omega \sin \varphi \sim \beta L$ , being

$f_0$  the Coriolis parameter and  $\beta = df/dy$ ,  $y$  is the North-South distance), the vertical velocity difference over one scale height is given by [20]:

$$\Delta u = \frac{R_g \Delta T}{\beta L^2} \quad (1)$$

where  $\beta = 2\Omega \cos \varphi / R_p = 5.35 \times 10^{-12} \text{ m}^{-1} \text{ s}^{-1}$  ( $\Omega = 1.64 \times 10^{-4} \text{ s}^{-1}$  is the angular frequency,  $\varphi = 10^\circ$  the latitude,  $R_p = 60330 \text{ km}$  the equatorial planetary radius) and  $R_g = 3886 \text{ J kg}^{-1} \text{ K}^{-1}$  (the specific gas constant). Using  $\Delta u \sim 200 \text{ m s}^{-1}$  (the 1980-81 to 1996-2004 velocity difference) and  $L \sim 12000 \text{ km}$  (the meridional distance between the maximum and minimum measured temperature difference across the equator), a North-South Equatorial temperature contrast  $\Delta T \sim 40 \text{ K}$  is obtained, which is 10 times that measured [16, 17]. Therefore it seems unrealistic to address the large  $200 \text{ m s}^{-1}$  difference in the wind speed solely to an altitude effect. A real change in the wind speed must have occurred close to the tropopause between the Voyager and HST-Cassini epochs. This change can account at least for  $\sim 100 \text{ m s}^{-1}$ , taking into account our error limits, with the other  $100 \text{ m s}^{-1}$  or less assigned to vertical wind shears. In fact, a signature of a dynamical change in the equatorial area between 1980-81 and 2004 could be present in the vertical wind shears derived from the Voyagers and Cassini temperature measurements. For example, according to Figure 3 in [15], in 1980-81 the winds increased with height above the 150 mbar level between latitudes  $10^\circ \text{ S}$  and  $25^\circ \text{ S}$  (and also between  $10^\circ \text{ N}$  and  $25^\circ \text{ N}$ ). On the contrary, during 2004, Flassar et al. (2005) [16] showed for the same altitude level that the winds decrease with altitude from  $5^\circ \text{ S}$  to  $15^\circ \text{ S}$ , remaining constant with altitude for latitudes between  $15^\circ \text{ S}$  to  $30^\circ \text{ S}$ . Although the spatial resolution of the temperature measurements differs between Voyager (about  $4^\circ$  in latitude) and Cassini (about  $8^\circ$  for the first published data [16]), the above data suggests that a significant dynamical change took place in the equatorial circulation at the tropopause level.

## 2.2 Wave motion

A second possibility to explain the wind speed difference is the existence of waves at cloud level during the HST-Cassini period, so the observed motions would not represent the real atmospheric mass flow but features formed by a wave (or a mixture of both) moving with phase speed  $c$  relative to a background flow with mean velocity  $\langle u \rangle$ . The blue and methane-band filtered HST images obtained during the period 1996-2004 shows patterns of large spots, periodically distributed in longitude, with zonal wavenumber  $n \sim 2 - 4$  centred usually at latitude  $10^\circ \text{ S}$ , reminiscent of a wave phenomena, Figure 1. Therefore adopting

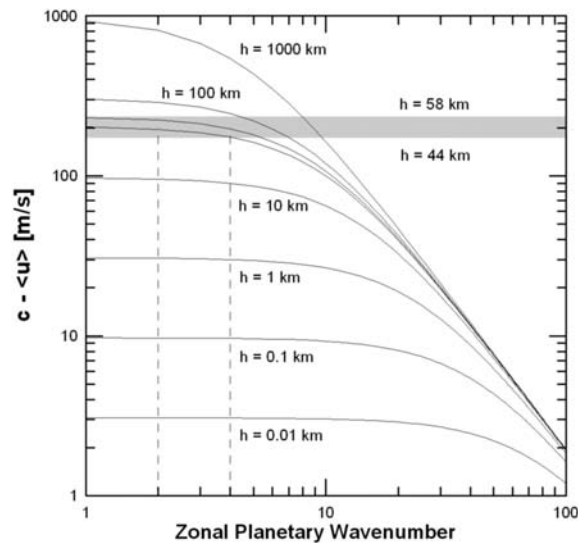


Figure 2: Dispersion relationship for Doppler shifted linear Equatorial Rossby waves as a function of the equivalent depth  $h$  (in  $km$ ). The horizontal band marks the values of  $h$  where the observations best fit this model.

$\langle u \rangle = 475 \text{ m s}^{-1}$  from the Voyager profile at this latitude, and assuming  $c = 275 \text{ m s}^{-1}$  from HST measurements, the relative velocity of the wave is  $c - \langle u \rangle \sim -200 \text{ m s}^{-1}$  (negative sign means westward relative motion). These waves could have been triggered by the large-scale storms that took place in 1990 and 1994 between  $5^\circ \text{ N}$  and  $10^\circ \text{ N}$  [9, 18]. Equatorial thermal waves were detected during the Voyagers encounters in near equatorial latitudes of Saturn (from  $10^\circ \text{ N}$  to  $20^\circ \text{ N}$ ) at the  $270 \text{ mbar}$  level [19]. Their zonal wave speed was dispersive with a high wavenumber ( $n = 22$ ) and a phase speed  $-216 \text{ m s}^{-1}$ , similar to that of the proposed waves at cloud level. Equatorial waves display different modes on Earth (see e.g. [20]) and in their linear form, they have been studied in Jupiter [21]. Since the spot pattern moved westward relative to the mean zonal flow, a good candidate would be an equatorial Rossby wave. According to [21], the dispersion relationship for Rossby waves is given by,

$$c - \langle u \rangle = \frac{-\beta R_p^2 / n^2}{1 + (2j + 1) \frac{\beta R_p^2}{n^2 \sqrt{gh}}} \quad (2)$$

Here  $g = 8.5 \text{ m.s}^{-2}$  is the gravity acceleration,  $h$  the equivalent depth or thickness of an incompressible fluid with the same horizontal properties and  $j$  is a meridional structure index. For the lowest mode ( $j = 1$ ) and for the values of the other parameters as given in the previous section, we plot in Figure 2 the dispersion relationship for different values of  $h$ . The best match to the observations occurs for equatorial Rossby waves with equivalent depths  $h \sim 44 - 58 \text{ km}$  or about  $1.5 H$ . According to our altitude analysis (clouds detected at a wavelength of  $890 \text{ nm}$  are at  $50 \text{ mbar}$  level), the waves should then extend in depth to the  $\sim 225 \text{ mbar}$  level. Alternatively, if one considers a  $100 \text{ m.s}^{-1}$  contribution due to the wind shear, then  $c - \langle u \rangle \sim 100 \text{ m.s}^{-1}$  and according to Figure 2 we get  $h = 10 \text{ km}$  (or  $0.25 H$ ). The Rossby waves can also act on the zonal mean flow accelerating or making it to decay upon the divergence of the Eliassen-Palm flux [19]. A careful analysis for wave search in the equatorial area using Cassini data will serve to assess this hypothesis for example adding new data points for other wavenumbers to the wave dispersion relationship of Figure 2.

### 2.3 Great Storm - Mean zonal flow interaction

The change in the equatorial jet took place following the development of a large-scale moist convective storm, the "Great White Spot" (GWS) in late September 1990 [9, 10], and after the subsequent intense cloud activity in this area along 1991 [22]. Four years later, in 1994, a second storm evolved northwards of the previous event [18], and was followed during 1997 by smaller scale storms [23]. Therefore it is reasonable to suppose that there could be a relationship between the storm activity and the jet variability. There are at least two possibilities for such interaction. The first one consists on the direct injection of momentum by the storm on the mean flow, following the conversion of thermal and potential energy in the storm to kinetic energy. The second one is indirect and is related to the injection of cloud and haze particles in the upper atmosphere by the storms, which should block the solar radiation, modifying the tropospheric temperatures and finally the dynamics. We examine the action of these two mechanisms on the equatorial jet.

#### Momentum injection by the Storm

As a first approach we use a moist (ammonia and water) one-dimensional convective model for the storm to estimate the vertical wind speed for an ascending parcel on a saturated environment [24]. Using the work-energy theorem, with the buoyancy force making the work along the ascending path, the vertical velocity within the storm is given by

$$w = \sqrt{2gx_c \left\{ \frac{L_c}{C_p T} - f_c \right\} H \ln \frac{P_0}{P_1}} \quad (3)$$

with  $x_c = 1.7 \times 10^{-3}$  the water mixing ratio (assumed to be solar), the latent heat of condensation  $L_c = 6306 \text{ J mol}^{-1}$ ,  $C_p = 30 \text{ J mol}^{-1} \text{ K}^{-1}$ ,  $T = 85 \text{ K}$ ,  $H = 38 \text{ km}$  and the pressure ranging from the water cloud at  $P_0 \sim 10 \text{ bar}$  to the tropopause at  $P_1 \sim 0.1 \text{ bar}$ . Maximum vertical velocities are attained if full precipitation of the condensate within the storm is assumed ( $f_c = 0$ ), producing very intense updrafts with  $w \sim 100 \text{ ms}^{-1}$ . The action of the Coriolis force on the ascending parcels within the storm along their large vertical path of  $\sim 300 \text{ km}$ , deflects them with a westward acceleration over the zonal flow

$$\frac{du}{dt} \approx -2\Omega w \cos \varphi \quad (4)$$

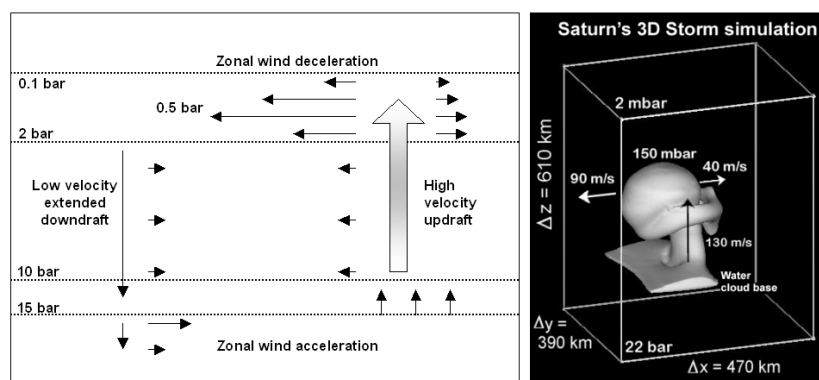


Figure 3: Schematic diagram of the zonal momentum production by a water moist convective storm from 3D simulations. Left: A powerful updraft subjected to Coriolis forces deflects westward all the way up to the  $100 \text{ mbar}$  (tropopause) with maximum divergence and negative (westward) momentum production at  $500 \text{ mbar}$ . Displaced air descends through much wider areas to deep levels increasing the zonal momentum. The result is wind decreasing at the upper stable levels and increasing below the water cloud base. Right: Model of a single convective cell from 3D calculations [25].

Accordingly, an uprising parcel could develop westward motions with maximum velocities of  $u \sim 100 \text{ ms}^{-1}$  in  $\sim 2 \text{ hrs}$  of ascension. More detailed three-dimensional simulations of water storms on Saturn [25], produce a net local

westward motions close to the upraising cumulus with speeds of  $\sim 50 \text{ m s}^{-1}$  as shown in Figure 3. The effect of ammonia storms can be neglected since they only develop vertical velocities  $w \sim 10 \text{ m s}^{-1}$  [24, 25]. Therefore, westward injection of momentum by powerful water storms in the upper troposphere, flowing on a direction contrary to the jet, can reduce significantly its eastward velocity.

### Temperature-dynamical changes induced by storm particles

Following the GWS development, a huge quantity of bright particles formed in the upper troposphere [26], most probably as a result of the condensation of fresh ammonia and water [25]. The measurements of brightness variations in the equatorial area, following the 1990 GWS, suggest that these particles transformed later in darker (more absorbing) and long-lived aerosols [27]. This aerosol layer could perturb the local temperature, inducing dynamical changes. Here we estimate under a linear approach, the expected magnitude of the wind speed variability induced by this mechanism. The thermodynamic equation, assuming hydrostatic conditions, is given by

$$\frac{\partial T}{\partial t} + \frac{N^2 H}{R_g/\mu} w = \frac{Q}{\rho C_p} \quad (5)$$

where  $\mu = 2.136 \text{ gmol}^{-1}$ ,  $N$  the Brunt-Väisälä frequency and  $w$  the vertical velocity. The heating rate  $Q$  (effective energy deposited per unit volume and time,  $W m^{-3}$ ) at the Equator has been estimated by [28] to be about  $2.3 \times 10^{-6} \text{ K s}^{-1}$  and takes place in the aerosol layer (tropospheric haze) located between  $\sim 60 - 200 \text{ mbar}$ . Let us estimate the contribution to the zonal wind change due to both terms in equation 5.

- Balancing the temperature change and the heating function terms in equation 5 allows to estimate the temperature disturbance introduced by the sunlight absorption in the aerosol layer  $\Delta T \approx \Delta t(Q/\rho C_p)$ . Assuming a cooling rate about half the above heating rate and taking both place along  $t \sim 1 \text{ yr}$ , we get a temperature increase at the equator  $T \sim 5 \text{ K}$  during this year. The thermal-wind equation 1 predicts a drop in the zonal with altitude of the order  $25 \text{ m s}^{-1}$ .
- On the other hand, assuming steady conditions, a balance between the dynamical and heating terms in equation 5 allows to calculate the upward velocity induced by such heating:

$$w \approx \frac{R_g/\mu}{N^2 H} \frac{Q}{\rho C_p} \quad (6)$$



and using  $N^2 \sim 6 \times 10^{-5} \text{ s}^{-2}$  at the tropopause yields a vertical velocity  $w \sim 0.0004 \text{ m s}^{-1}$ , which as expected is much lower than the vertical motions produced by moist convection. From the mass continuity, the expected change in the zonal velocity will be  $u \sim w(L/H) \sim -1 \text{ m s}^{-1}$  ( $H$  is the scale height equal to  $38 \text{ km}$  at the Equator).

From this discussion, we conclude according to equation 5, that the temperature increase at the Equator (and its meridional gradient) should be much more effective than the induced vertical motion in changing the zonal winds, but still far enough to explain a  $200 \text{ m s}^{-1}$  drop.

## 2.4 Atmospheric Angular Momentum Change

Finally, we explore if a true wind velocity change involving the upper atmospheric cloud layers (above water clouds,  $P < 12 \text{ bar}$ ), could produce a detectable change in the rotation period of the planet. The problem is of interest in view of the recently reported change in the radio rotation period [29, 30]. The conservation of the total angular momentum of the planet implies that if a change in the atmospheric angular momentum  $L_{atm}$  occurs, then the rotation rate (angular velocity) of the planet  $\Omega_p$  (period  $\tau_p$ ) must change according to

$$\delta\Omega_p = \frac{\delta L_p}{I_p} = -\frac{\delta L_{atm}}{I_p} \quad (7)$$

being  $L_p$  and  $L_{atm}$  the angular momentum of the planet and atmosphere respectively and  $I_p = 9.12506 \times 10^{40} \text{ kg m}^2$  the principal momentum of inertia of Saturn. Defining  $L_{atm} = I_{atm} \delta\Omega_{atm}$ , where  $I_{atm}$  is the atmospheric momentum of inertia and  $\delta\Omega_{atm} \sim \delta u/R_p$ , we get

$$\delta u = R_p \Omega_p^2 \frac{\delta\tau_p}{2\pi} \frac{I_p}{I_{atm}} \quad (8)$$

Using for  $\Omega_p$  the System III Voyager radio rotation period [31], we get

$$\delta u = 0.256 \delta\tau_p \frac{I_p}{I_{atm}} (\text{m s}^{-1}) \quad (9)$$

Taking  $\delta u = -200 \text{ m s}^{-1}$  (the change in wind velocity between the Voyager and HST periods), the accompanying change in the rotation period of the planet would be,

$$\delta\tau_p(s) = -781.25 \frac{I_{atm}}{I_p} \quad (10)$$

To estimate the period change we assume that the atmospheric mass involved in the velocity is that located above the water clouds within the layer sheet bounded in latitude between  $20^\circ$  N and  $20^\circ$  S. Its mass is then given by  $M_{atm} \sim P_0 S/g$  ( $P_0 \sim 12$  bar and  $S$  is the area between these two latitudes) yielding  $I_{atm} \sim 10^{-4} I_p$ , and from equation 10 we get  $\delta\tau_p \sim 0.12$  s, which is well below the level of the precision of the measurement of the rotation period by the radio emission modulation. Note that the 6 minute change observed in the radio rotation period between the Voyagers visit and the Ulysses and Cassini measurements [29], cannot be explained in this simple way since: (a) the low values involved; (b) it goes in the opposite direction, i.e. a decrease in the planetary period will produce an increase in the atmospheric wind speed.

### 3 Conclusion

We have shown that the wind variability so far reported on Saturn's equatorial area cannot be due solely to a vertical wind shear effect, in agreement with our previous study on cloud altitudes in 1980-81 and 1996-2004 [1]. Our analysis suggests that in addition to a vertical wind shear (decreasing winds with altitude below the upper clouds), dynamical mechanisms should have been involved. The layer affected by this variability is most probably confined to the upper troposphere, in or above the ammonia cloud condensation level (1.5 – 2 bar) where waves or westward momentum injection are more effective. We also rule out a possible relationship between this wind variability and the detected radio-rotation period increase from 1980-81 to 1996-2004. Careful studies with the different instruments onboard Cassini spacecraft should improve significantly our knowledge of this problem.

*Acknowledgements:* ASL and SPH were supported by the research projects AYA2003-03216, FEDER and Grupos UPV 15946/2004. RH was supported through the Ramón y Cajal program of Spanish MEC.

### References

- [1] Pérez-Hoyos, S., Sánchez-Lavega, A. 2006, *Icarus* 180, 161

- [2] Sánchez-Lavega, A., Hueso, R., Pérez-Hoyos, S., García-Melendo, E., Rojas, J.F. 2004, *Lecture Notes and Essays in Astrophysics I*, pg. 63, Ed. A. Ulla and M. Manteiga (RSEF), Gamesal, Vigo
- [3] Ingersoll, A.P., Dowling, T.E., Gierasch, P.J., Orton, G.S., Read, P.L., Sánchez-Lavega, A., Showman, A.P., Simon-Miller, A.A., Vasavada, A.R. 2004, in *Jupiter :The Planet, Satellites, and Magnetosphere*, F. Bagenal, T.E. Dowling and W. McKinnon, Eds. Cambridge University Press, p. 180
- [4] Vasavada, A.R., Showman, A. 2005, *Rep. Prog. Phys.* 68, 1935.
- [5] Barnet, C.D., Beebe, R.F., Conrath, B.J. 1992, *Icarus* 98, 94
- [6] Yamazaki, Y.H., Read, P. L., Skeet, D. R. 2005, *Planet. Space Sci.* 53, 508
- [7] Arnou, J.M., Heimpel, M. H. 2004, *Icarus* 169, 492
- [8] Sánchez-Lavega, A., Pérez-Hoyos, S., Hueso, R., Rojas, J.F., French, R.G. 2003, *Nature* 423, 623
- [9] Sánchez-Lavega, A., Colas, F., Lecacheux, J., Laques, P., Miyazaki, I., Parker, D. 1991, *Nature* 353, 397
- [10] Barnet, C.D., Westphal, J.A., Beebe, R.F., Huber, L.F. 1992, *Icarus* 100, 499
- [11] Porco, C.C. et al. 2005, *Science* 307, 1243
- [12] Ingersoll, A.P., Beebe, R. F. , Conrath, B. J., Hunt, G. E. 1984, in *Saturn*, T.Gehrels and M. S. Matthews (eds.), University of Arizona Press, Tucson, p. 195
- [13] Sánchez-Lavega, A., Rojas, J.F., Sada, P.V. 2000, *Icarus* 147, 405
- [14] Sánchez-Lavega, A., Hueso, R., Pérez-Hoyos, S., Rojas, J. F., French, R.G. 2004, *Icarus* 170, 519
- [15] Conrath, B.J., Pirraglia, J.A. 1983, *Icarus* 53, 286
- [16] Flasar, F.M. et al. 2005, *Science* 307, 1247
- [17] Orton, G.S., Yanamandra-Fisher, P.A. 2005, *Science* 307, 696
- [18] Sánchez-Lavega, A., Lecacheux, J., Gomez, J.M., Colas, F., Laques, P., Noll, K., Gilmore, D., Miyazaki, I., Parker, D. 1996, *Science* 271, 631
- [19] Achterberg, R.K., Flasar, F.M. 1996, *Icarus* 119, 350
- [20] Andrews, D.G. , Holton, J.R., Leovy, C.B. 1987, in *Middle Atmosphere Dynamics*, Academic Press
- [21] Allison, M. 1990, *Icarus* 83, 282
- [22] Sánchez-Lavega, A., Lecacheux, J., Colas, F., Laques, P. 1993, *Journal of Geophysical Research* 98, 18857
- [23] Sánchez-Lavega, A., Lecacheux, J., Gomez, J.M., Colas, F., Rojas, J.F., Gez, J.M. 1999, *Planet. Space Scien.* 47, 1277
- [24] Sánchez-Lavega, A., Battaner, E. 1987, *A&A* 185, 315
- [25] Hueso, R., Sánchez-Lavega, A. 2004, *Icarus* 172, 255
- [26] Acarreta, J.R., Sánchez-Lavega, A. 1999, *Icarus* 137, 24
- [27] Pérez-Hoyos, S., Sánchez-Lavega, A., French, R., Rojas, J.F. 2005, *Icarus* 176, 155
- [28] Pérez-Hoyos, S., Sánchez-Lavega, A., French, R., Rojas, J.F. 2006, *Icarus* 180, 368
- [29] Gurnett, D.A. et al. 2005, *Science* 307, 1255
- [30] Sánchez-Lavega, A. 2005, *Science* 307, 1223
- [31] Seidelmann, P.K. et al. 2002, *Cel Mech. & Dyn. Astron.* 82, 83

